

## Manganese Porphyrins as Redox-Coupled Peroxynitrite Reductases

Jinbo Lee, Julianne A. Hunt, and John T. Groves\*

Contribution from the Department of Chemistry, Princeton University, Princeton, New Jersey 08544

Received January 9, 1998

**Abstract:** Superoxide ( $O_2^{\bullet-}$ ) and peroxynitrite ( $ONOO^-$ ) have been implicated in many pathophysiological conditions. To develop novel catalysts that have both  $ONOO^-$  decomposition and  $O_2^{\bullet-}$  dismutase activity, and to understand the mechanisms of these processes, we have explored the reactivity of 5,10,15,20-tetrakis(*N*-methyl-4'-pyridyl)porphinatomanganese(III) [Mn(III)TMPyP] toward  $ONOO^-$  and  $O_2^{\bullet-}$ . The reaction of Mn(III)TMPyP with  $ONOO^-$  to generate an oxomanganese(IV) porphyrin species [(oxoMn(IV))] is fast, but Mn(III)TMPyP is not catalytic for  $ONOO^-$  decomposition because of the slow reduction of oxoMn(IV) back to the Mn(III) oxidation state. However, biological antioxidants such as ascorbate, glutathione, and Trolox rapidly turn over the catalytic cycle by reducing oxoMn(IV). Thus, Mn(III)TMPyP becomes an efficient peroxynitrite reductase when coupled with ascorbate, glutathione, and Trolox ( $k_c \approx 2 \times 10^6 M^{-1} s^{-1}$ ), though the direct reactions of  $ONOO^-$  with these biological antioxidants are slow ( $88 M^{-1} s^{-1}$ ,  $5.8 \times 10^2 M^{-1} s^{-1}$ , and  $33 M^{-1} s^{-1}$ , respectively). Mn(III)TMPyP is known to catalyze the dismutation of  $O_2^{\bullet-}$ , and using stopped-flow spectrophotometry, the rate of Mn(III)TMPyP-catalyzed dismutation has been measured directly ( $k_c = 1.1 \times 10^7 M^{-1} s^{-1}$ ). Further,  $O_2^{\bullet-}$ , like the biological antioxidants, rapidly reduces oxoMn(IV) to the Mn(III) oxidation state ( $k \approx 10^8 M^{-1} s^{-1}$ ), transforming Mn(III)TMPyP into a  $O_2^{\bullet-}$ -coupled  $ONOO^-$  reductase. Under conditions of oxidative stress and reduced antioxidant levels, Mn(III)TMPyP may deplete  $O_2^{\bullet-}$  primarily as a function of its  $ONOO^-$  reductase activity, and not through its  $O_2^{\bullet-}$  dismutase activity.

## Introduction

The reactive oxygen species superoxide ( $O_2^{\bullet-}$ ) and peroxynitrite ( $ONOO^-$ ) have been implicated as important mediators of tissue injury and cellular dysfunction under conditions of toxic shock, inflammation, and oxidative stress.<sup>1,2</sup> Although a large flux of  $O_2^{\bullet-}$  is produced by aerobic metabolism (1–5% of total oxygen consumption is estimated to be reduced to  $O_2^{\bullet-}$ ),<sup>3</sup> the concentration of  $O_2^{\bullet-}$  is maintained at very low levels by the superoxide dismutase (SOD) enzymes, which are found at micromolar intracellular concentrations. These metalloenzymes react with  $O_2^{\bullet-}$  at rates in the range  $10^8 M^{-1} s^{-1}$  for mitochondrial MnSOD<sup>4</sup> and at the near-diffusion-limited rate of  $2 \times 10^9 M^{-1} s^{-1}$  for Cu,ZnSOD.<sup>5</sup> The reaction rate for the formation of  $ONOO^-$  from  $O_2^{\bullet-}$  and nitric oxide ( $NO^\bullet$ ) is even faster at  $6.7 \times 10^9 M^{-1} s^{-1}$ .<sup>6,7</sup> Thus, when the level of  $NO^\bullet$  rises to micromolar concentrations—as it does, for example, during cerebral ischemia and near activated macrophages— $NO^\bullet$  can effectively compete with SOD for  $O_2^{\bullet-}$ .<sup>2</sup> Accordingly,  $O_2^{\bullet-}$ , which may be toxic in its own right, is also efficiently converted into  $ONOO^-$ , an even more powerful oxidant, which is expected to have free access to cell interiors by virtue of its ability to cross phospholipid membranes.<sup>8</sup> For these reasons,  $ONOO^-$  may play a major role in a wide variety of human diseases.

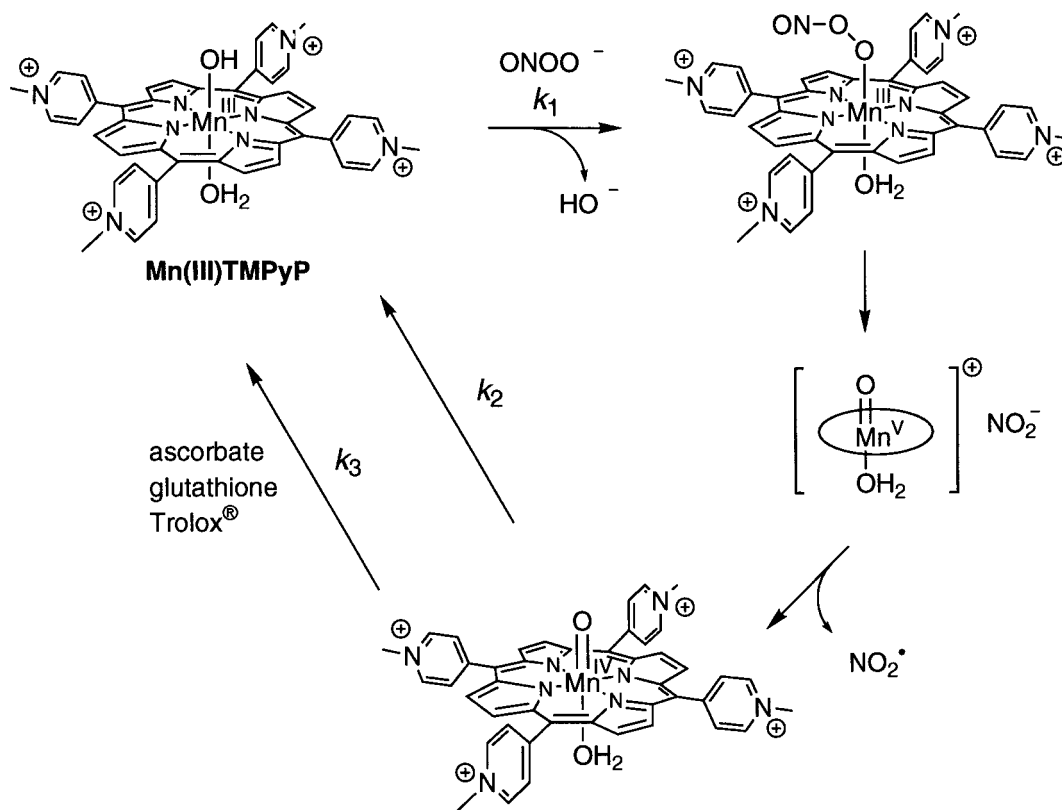
Administration of SOD enzymes has been shown to provide protection from tissue damage associated with various types of inflammatory diseases,<sup>1</sup> but the limitations associated with using enzymes for pharmaceutical intervention (e.g., bioavailability, stability) have motivated a search for synthetic SOD mimics of low molecular weight. For example, Riley et al. have developed a series of manganese complexes that effectively catalyze the dismutation of  $O_2^{\bullet-}$ .<sup>9,10</sup> These agents inhibit neutrophil-mediated cell injury *in vitro*<sup>11</sup> and neutrophil-mediated tissue injury *in vivo*.<sup>12</sup> Similarly, synthetic catalysts for fast  $ONOO^-$  decomposition may have important therapeutic applications, and Stern et al. recently discovered that the water-soluble iron porphyrins, 5,10,15,20-tetrakis(*N*-methyl-4'-pyridyl)porphinatoiron(III) [Fe(III)TMPyP] and 5,10,15,20-tetrakis(2,4,6-trimethyl-3,5-sulfonatophenyl)porphinatoiron(III) [Fe(III)TMPS] function as “peroxynitrite isomerases” to catalyze the rapid isomerization of  $ONOO^-$  to  $NO_3^-$ .<sup>13</sup> These iron porphyrins demonstrated profound activity in  $ONOO^-$  related disease models.<sup>14,15</sup>

Our recent discovery that Mn(III)TMPyP shows high reactivity with  $ONOO^-$ <sup>8,16</sup> has prompted us to explore the development of novel catalysts with the potential for high  $ONOO^-$  decomposition and  $O_2^{\bullet-}$  dismutation activity through an understanding of the mechanisms and kinetics of these processes. The

\* To whom correspondence should be addressed.

- Halliwell, B.; Gutteridge, J. M. C. *Methods Enzymol.* **1990**, *186*, 1.
- Beckman, J. S.; Koppenol, W. H. *Am. J. Physiol.* **1996**, *271*, C1424.
- Imlay, J. A.; Fridovich, I. *J. Biol. Chem.* **1991**, *266*, 6957.
- Gray, B.; Carmichael, A. J. *Biochem. J.* **1992**, *281*, 795.
- Fridovich, I. *J. Biol. Chem.* **1989**, *264*, 7761.
- Huie, R. E.; Padmaja, S. *Free Radical. Res. Commun.* **1993**, *18*, 195.
- Recently, it has been shown that the reaction rate for the formation of  $ONOO^-$  from  $O_2^{\bullet-}$  and  $NO^\bullet$  is even faster, at  $1.9 \times 10^{10} M^{-1} s^{-1}$  (Kissner, R.; Nauser, T.; Bugnon, P.; Lye, P. G.; Koppenol, W. H. *Chem. Res. Toxicol.* **1997**, *10*, 1285).
- Marla, S. S.; Lee, J.; Groves, J. T. *Proc. Natl. Acad. Sci. U.S.A.* **1997**, *94*, 14243.

- Riley, D. P.; Weiss, R. H. *J. Am. Chem. Soc.* **1994**, *116*, 387.
- Riley, D. P.; Lennon, P. J.; Neumann, W. L.; Weiss, R. H. *J. Am. Chem. Soc.* **1997**, *119*, 6522.
- Hardy, M. M.; Flickinger, A. G.; Riley, D. P.; Weiss, R. H.; Ryan, U. S. *J. Biol. Chem.* **1994**, *269*, 18535.
- Weiss, R. H.; Fretland, D. J.; Baron, D. A.; Ryan, U. S.; Riley, D. P. *J. Biol. Chem.* **1996**, *271*, 26149.
- Stern, M. K.; Jensen, M. P.; Kramer, K. *J. Am. Chem. Soc.* **1996**, *118*, 8735.
- Stern, M. K.; Salvemini, D. *PCT Int. Appl. WO95/31197*, 1995.
- Salvemini, D.; Wang, Z. Q.; Stern, M. K.; Currie, M. G.; Misko, T. P. *Proc. Natl. Acad. Sci. U.S.A.* **1998**, *95*, 2659–2663.

Scheme 1<sup>a</sup>

<sup>a</sup>  $k_1 = 1.8 \times 10^6 \text{ M}^{-1} \text{ s}^{-1}$ ;  $k_2 = 0.018 \text{ s}^{-1}$ ;  $k_3 = 5.4 \times 10^7$ ,  $1.3 \times 10^5$ , and  $7.0 \times 10^6 \text{ M}^{-1} \text{ s}^{-1}$  for ascorbate, glutathione, and Trolox, respectively. As described in the text and figure legends, all rates were determined at 23 °C in 50 mM phosphate buffer, pH 7.4.

manganese porphyrin Mn(III)TMPyP has been shown by indirect assay to catalyze the dismutation of  $\text{O}_2^{\bullet-}$  at a rate of  $\sim 10^7 \text{ M}^{-1} \text{ s}^{-1}$ ,<sup>17</sup> and both Mn(III)TMPyP and the structurally related synthetic porphyrin 5,10,15,20-tetrakis(4-benzoic acid)-porphyrinatomanganese(III) [Mn(III)TBAP] have proved effective in protecting cells against oxidative stress.<sup>17–20</sup>

At a first glance, the protective ability of Mn(III)TMPyP<sup>17–20</sup> is puzzling. Although the rate of  $\text{O}_2^{\bullet-}$  dismutation catalyzed by Mn(III)TMPyP ( $\sim 10^7 \text{ M}^{-1} \text{ s}^{-1}$ ) is rapid, that rate translates into only  $\sim 1\%$  of the activity of native SOD on a molar basis.<sup>5</sup> Similarly, the high reactivity of Mn(III)TMPyP with  $\text{ONOO}^-$ <sup>8,16</sup> does not translate directly into high  $\text{ONOO}^-$  decomposition activity. As we have shown,  $\text{ONOO}^-$  rapidly oxidizes Mn(III)TMPyP to an oxoMn(IV) species, but Mn(III)TMPyP alone is not catalytic for  $\text{ONOO}^-$  decomposition due to the slow reduction of oxoMn(IV) back to the Mn(III) oxidation state.<sup>21</sup> Fridovich et al. have suggested that Mn(III)TMPyP is reduced to the Mn(II) state in vivo, at the expense of NADPH or glutathione. Since the Mn(II) porphyrin can be reoxidized to Mn(III)TMPyP by  $\text{O}_2^{\bullet-}$  with a rate constant of  $4 \times 10^9 \text{ M}^{-1} \text{ s}^{-1}$ ,<sup>22</sup> it was proposed that the protective effects of Mn(III)TMPyP in vivo stem from its activity as a reductant:  $\text{O}_2^{\bullet-}$  oxidoreductase rather than as a  $\text{O}_2^{\bullet-}$  dismutase.<sup>17</sup> Our recent

results<sup>23</sup> also reveal that Mn(III)TMPyP can demonstrate profound changes in activity in the presence of biological reductants.

Here we report an elucidation of the mechanisms and kinetics of the reactions of  $\text{O}_2^{\bullet-}$  and  $\text{ONOO}^-$  with Mn(III)TMPyP. Specifically, we have found that Mn(III)TMPyP becomes a highly effective peroxynitrite reductase<sup>24</sup> when redox coupled with the biological antioxidants ascorbate, glutathione, and Trolox (a water-soluble analogue of  $\alpha$ -tocopherol), which rapidly reduce oxoMn(IV) back to the Mn(III) oxidation state (see Scheme 1). We have also measured the rate of Mn(III)TMPyP-catalyzed  $\text{O}_2^{\bullet-}$  dismutation directly for the first time, using stopped-flow spectrophotometry, and our results are in agreement with the published rates determined by indirect assay<sup>17</sup> and pulse radiolysis.<sup>22</sup> Further, we have investigated the interactions between Mn(III)TMPyP,  $\text{ONOO}^-$ , and  $\text{O}_2^{\bullet-}$ , and we have discovered that  $\text{O}_2^{\bullet-}$ , like the biological antioxidants, can rapidly reduce oxoMn(IV)TMPyP to the Mn(III) oxidation state, transforming Mn(III)TMPyP into a *superoxide-coupled peroxynitrite reductase*. Significantly, the results described here indicate that Mn(III)TMPyP will deplete  $\text{O}_2^{\bullet-}$  primarily as a function of a  $\text{ONOO}^-$  coupled pathway at biologically relevant ratios of  $\text{O}_2^{\bullet-}$  and  $\text{ONOO}^-$ . This surprising result would explain the high biological activity of MnTMPyP.

## Results and Discussion

We have shown that the water-soluble manganese porphyrin, Mn(III)TMPyP, is an excellent marker for  $\text{ONOO}^-$  due to the

(23) Lee, J.; Hunt, J. A.; Groves, J. T. *Bioorg. Med. Chem. Lett.* **1997**, 7, 2913.

(24) While the term *peroxynitrite reductase* has been used here, it should be noted that the general nature of the reaction is analogous to *peroxidase* activity.

(16) Groves, J. T.; Marla, S. S. *J. Am. Chem. Soc.* **1995**, 117, 9578.

(17) Faulkner, K. M.; Liochev, S. I.; Fridovich, I. *J. Biol. Chem.* **1994**, 269, 23471.

(18) Gardner, P. R. *Arch. Biochem. Biophys.* **1996**, 333, 267.

(19) Gardner, P. R.; Nguyen, D. H.; White, C. W. *Arch. Biochem. Biophys.* **1996**, 325, 20.

(20) Szabo, C.; Day, B. J.; Salzman, A. L. *FEBS Lett.* **1996**, 381, 82.

(21) Groves, J. T.; Lee, J.; Marla, S. S. *J. Am. Chem. Soc.* **1997**, 119, 6269.

(22) Faraggi, M. In *Oxygen Radicals in Chemistry and Biology*; Bors, W., Saran, M., Tait, D., Eds.; Walter de Gruyter: Berlin, Germany, 1984; pp 419–430.

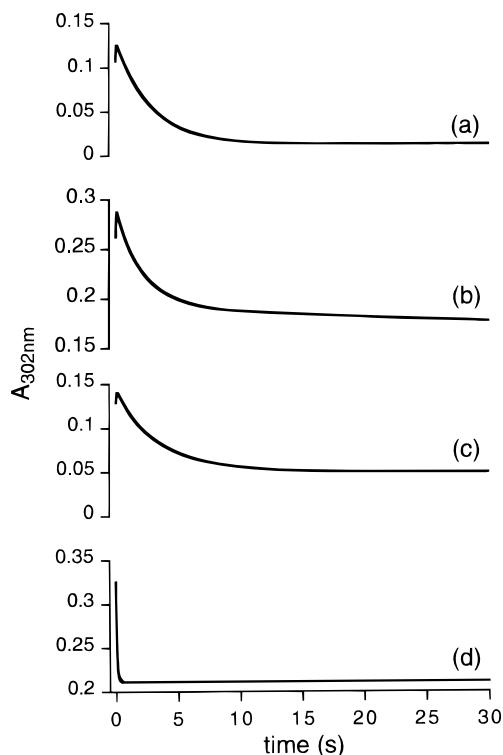


**Figure 1.** Decomposition of 100  $\mu\text{M}$  ONOO<sup>-</sup> monitored at 302 nm: (a) in 25 mM pH 7.4 phosphate buffer at 25 °C, with a first-order rate of 0.35 s<sup>-1</sup>; (b) in the presence of 10  $\mu\text{M}$  Mn(III)TMPyP, with a rate of 0.35 s<sup>-1</sup>; (c) in the presence of 100  $\mu\text{M}$  ascorbate, with a first-order rate of 0.29 s<sup>-1</sup>; (d) in the presence of 10  $\mu\text{M}$  Mn(III)TMPyP and 150  $\mu\text{M}$  ascorbate, with a rate of 22.4 s<sup>-1</sup>.

diagnostic formation of an oxoMn(IV) intermediate.<sup>8,16</sup> The reaction of Mn(III)TMPyP with ONOO<sup>-</sup> to generate oxoMn(IV) is among the fastest reactions known for ONOO<sup>-</sup>,<sup>25</sup> with a second-order rate constant of  $1.8 \times 10^6 \text{ M}^{-1} \text{ s}^{-1}$ .<sup>8</sup> Nevertheless, Mn(III)TMPyP is not an efficient catalyst for ONOO<sup>-</sup> decomposition because of the relative stability of oxoMn(IV).

In typical experiments, rates of ONOO<sup>-</sup> decomposition were measured with stopped-flow spectrophotometry by monitoring the ONOO<sup>-</sup> absorbance at 302 nm. As shown in Figure 1, the presence of 10  $\mu\text{M}$  Mn(III)TMPyP did not significantly accelerate the spontaneous decay of ONOO<sup>-</sup> at pH 7.4 (Figure 1b). Similarly, ascorbate alone did not significantly affect this spontaneous reaction (Figure 1c). However, the incorporation of near stoichiometric amounts of ascorbate with the manganese porphyrin dramatically reduced the half-life ( $t_{1/2}$ ) of ONOO<sup>-</sup> ~70-fold, from 2 s to 0.03 s (Figure 1d).

**Peroxyntirite Decomposition by the Mn(III)TMPyP–Ascorbate Redox Couple.** The direct uncatalyzed reaction of ONOO<sup>-</sup> with ascorbate was found to be slow, first order in ONOO<sup>-</sup>, and first order in ascorbate. The apparent first-order rate constant for ONOO<sup>-</sup> depletion, as determined by stopped-flow spectrophotometry, correlated linearly with the concentration of ascorbate under pseudo-first-order conditions (excess ascorbate), yielding a second-order rate constant of  $88 \text{ M}^{-1} \text{ s}^{-1}$  at 25 °C in 25 mM pH 7.4 phosphate buffer (Figure 2a). This is consistent with the results of Bartlett et al. and further supports the notion that ascorbate alone cannot play a significant direct role in the defense against ONOO<sup>-</sup>.<sup>26</sup>

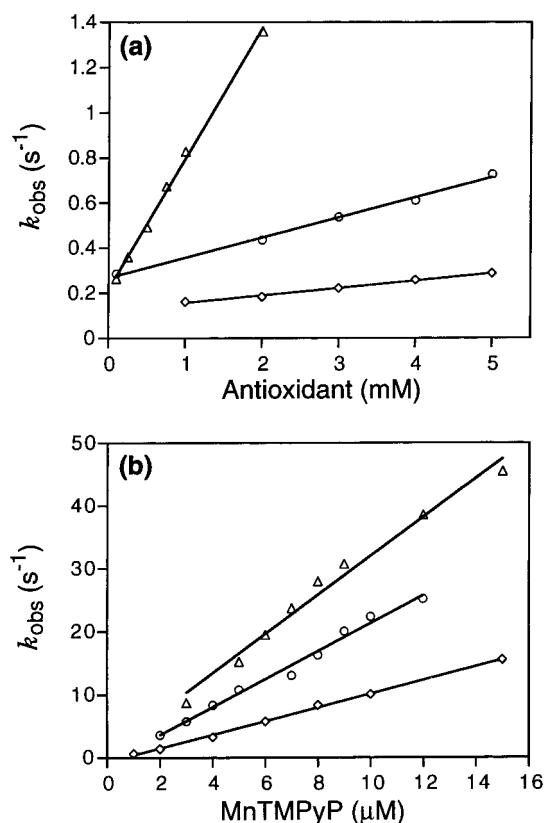


**Figure 2.** (a) Plot of the apparent first-order rate ( $k_{\text{obs}}$ ) of the reaction between ONOO<sup>-</sup> and antioxidants such as ascorbate (○), glutathione (Δ), and Trolox (◇) under pseudo-first-order conditions vs the concentrations of these antioxidants. Linear least-squares fitting of the experimental data yielded a second-order rate constant of 88 ( $R = 0.997$ ),  $5.8 \times 10^2$  ( $R = 0.997$ ), and  $33 \text{ M}^{-1} \text{ s}^{-1}$  ( $R = 0.994$ ) for ascorbate, glutathione, and Trolox, respectively. (b) ONOO<sup>-</sup> decomposition catalyzed by various concentrations of Mn(III)TMPyP in the presence of biologically significant concentrations of antioxidants [150  $\mu\text{M}$  ascorbate (○), 2 mM glutathione (Δ), or 150  $\mu\text{M}$  Trolox (◇)]. Antioxidants were added to the Mn(III)TMPyP solutions immediately before the stopped-flow experiments to minimize the slow autoxidation of antioxidants catalyzed by Mn(III)TMPyP under air. The apparent first-order rates correlated linearly with the catalyst concentrations with  $k_c$  of  $2.2 \times 10^6$  ( $R = 0.994$ ),  $3.2 \times 10^6$  ( $R = 0.992$ ), and  $1.1 \times 10^6 \text{ M}^{-1} \text{ s}^{-1}$  ( $R = 0.999$ ) for ascorbate, glutathione, and Trolox, respectively.

In marked contrast, Mn(III)TMPyP efficiently utilized ascorbate as the electron source for the reduction of ONOO<sup>-</sup>, displaying peroxyntirite reductase activity (Figure 2b). The turnover rate of the Mn(III)TMPyP-catalyzed decomposition of ONOO<sup>-</sup> in the presence of 1.5 equiv of ascorbate was dependent on the concentration of the catalyst (Figure 2b). The catalytic rate constant ( $k_c$ ) was determined to be  $2.2 \times 10^6 \text{ M}^{-1} \text{ s}^{-1}$ , which is nearly equivalent to the formation rate of oxoMn(IV) by ONOO<sup>-</sup>.<sup>8</sup> This suggests that oxoMn(IV) formation becomes the rate-limiting step in the catalytic cycle of ONOO<sup>-</sup> decomposition when ascorbate is present (Scheme 1).

**Reduction of OxoMn(IV) by Ascorbate.** Mn(III)TMPyP does not catalyze ONOO<sup>-</sup> decomposition in the absence of ascorbate because the conversion of oxoMn(IV) back to Mn(III) to complete the catalytic cycle has a first-order rate constant of  $\sim 0.018 \text{ s}^{-1}$ , much slower than the spontaneous decay of ONOO<sup>-</sup> (0.35 s<sup>-1</sup>) under these conditions (Figure 3a).<sup>21</sup> As we have recently shown,<sup>21</sup> the oxidation of Mn(III)TMPyP by HSO<sub>5</sub><sup>-</sup> rapidly and stoichiometrically forms an oxoMn(IV) intermediate via an oxoMn(V) precursor. We have measured the rate of reduction of oxoMn(IV) to Mn(III) by ascorbate in

(25) Floris, R.; Piersma, S. R.; Yang, G.; Jones, P.; Wever, R. *Eur. J. Biochem.* **1993**, *215*, 767.

(26) Bartlett, D.; Church, D. F.; Bounds, P. L.; Koppenol, W. H. *Free Radical. Biol. Med.* **1995**, *18*, 85.

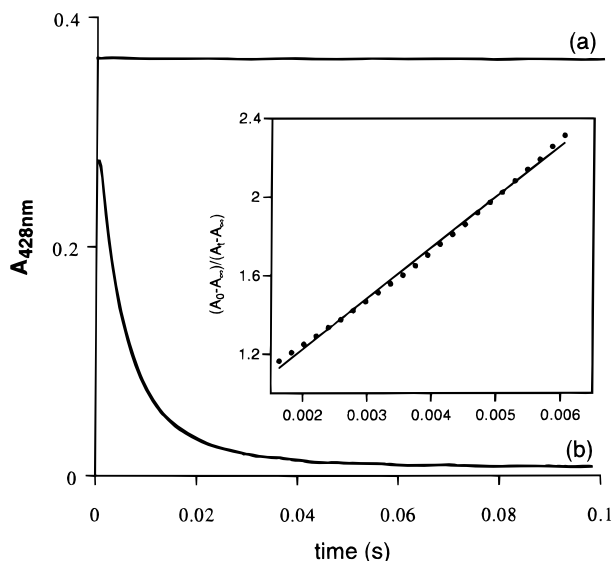


**Figure 3.** Double-mixing stopped-flow experiments to determine the rate of reduction of the oxoMn(IV) intermediate by ascorbate, in which Mn(III)TMPyP was first mixed with  $\text{HSO}_5^-$  to generate  $10 \mu\text{M}$  oxoMn(IV) and (a) pH 7.4 phosphate buffer or (b)  $10 \mu\text{M}$  ascorbate was then added in the second mixing step after a 5 s age time, to provide final concentrations of  $5 \mu\text{M}$  MnTMPyP and  $5 \mu\text{M}$  ascorbate. The disappearance of oxoMn(IV) was monitored at 428 nm, and the appearance of Mn(III) was monitored at 462 nm; for clarity, only the traces at 428 nm are shown. Inset: A second-order analysis of the reaction of  $10 \mu\text{M}$  oxoMn(IV) and  $10 \mu\text{M}$  ascorbate, monitored at 462 nm, in which  $(A_0 - A_\infty)/(A - A_\infty)$  was plotted against time. Linear least-squares fitting of the plot gave a second-order rate constant of  $5.4 \times 10^7 \text{ M}^{-1} \text{ s}^{-1}$  ( $R = 0.998$ ).

a double-mixing experiment. When the oxoMn(IV) intermediate was generated by mixing Mn(III)TMPyP with 1 equiv of  $\text{HSO}_5^-$ , subsequent addition of 1 equiv of ascorbate greatly enhanced the reduction of oxoMn(IV) to Mn(III) (Figure 3b). The kinetic trace monitored at 428 nm shows the reduction of oxoMn(IV). Both nonlinear regression fitting of the trace at 462 nm and second-order kinetic analysis of the trace at 428 nm gave a second-order rate constant of  $5.4 \times 10^7 \text{ M}^{-1} \text{ s}^{-1}$  for the reduction of oxoMn(IV) by ascorbate (Figure 3b inset). This rapid reduction results in the peroxynitrite reductase activity of Mn(III)TMPyP, which is only limited by the rate of oxoMn(IV) formation in the catalytic cycle ( $k_1$  in Scheme 1).

**Glutathione and Trolox as Mn(III)TMPyP-Coupled Antioxidants.** Glutathione and Trolox were examined as candidates for redox coupling with Mn(III)TMPyP for the catalytic decomposition of  $\text{ONOO}^-$ . The direct reactions of  $\text{ONOO}^-$  with glutathione and Trolox are relatively slow, as in the case of ascorbate (Figure 2a). The second-order rate constants are  $5.8 \times 10^2$  and  $33 \text{ M}^{-1} \text{ s}^{-1}$  for glutathione and Trolox, respectively. Both antioxidants rapidly reduced oxoMn(IV) to Mn(III)TMPyP, with second-order rate constants of  $1.3 \times 10^5 \text{ M}^{-1} \text{ s}^{-1}$  for glutathione and  $7.0 \times 10^6 \text{ M}^{-1} \text{ s}^{-1}$  for Trolox (Table 1); thus, both of these reducing agents effectively complete the catalytic cycle of  $\text{ONOO}^-$  decomposition shown in Scheme 1. Interestingly, the rates of oxoMn(IV) reduction by ascorbate, Trolox, and glutathione follow the order of the reduction potentials of these biological antioxidants.<sup>27</sup>

Mn(III)TMPyP catalyzed the rapid decomposition of  $\text{ONOO}^-$  in the presence of physiologically significant concentrations of glutathione (2 mM) and Trolox (150  $\mu\text{M}$ ), with catalytic rate constants ( $k_c$ ) of  $3.2 \times 10^6$  and  $1.1 \times 10^6 \text{ M}^{-1} \text{ s}^{-1}$ , respectively

**Table 1.** Kinetic Evaluation of Mn(III)TMPyP-antioxidant Redox Couples for the Decomposition of  $\text{ONOO}^-$

antioxidant	$k_{\text{ONOO}^- + \text{antioxidant}}$ ( $\text{M}^{-1} \text{ s}^{-1}$ )	$k_{\text{Mn(IV)} \rightarrow \text{Mn(III)}}$ ( $\text{M}^{-1} \text{ s}^{-1}$ )	$k_c$ ( $\text{M}^{-1} \text{ s}^{-1}$ )
none	0.018 $\text{s}^{-1}$		
ascorbate	88	$5.4 \times 10^7$	$2.2 \times 10^6$
glutathione	$5.8 \times 10^2$	$1.3 \times 10^5$ <sup>b</sup>	$3.2 \times 10^6$
Trolox	33 <sup>a</sup>	$7.0 \times 10^6$ <sup>c</sup>	$1.1 \times 10^6$

<sup>a</sup> In all the Trolox reactions,  $\text{ONOO}^-$  decay was monitored at 289 nm to avoid interference from the Trolox phenoxyl radical and quinone interconversion (289 nm is the isosbestic point). <sup>b</sup> The rate of oxoMn(IV) reduction by glutathione was determined by a double-mixing stopped-flow experiment similar to that described for ascorbate (see text). The second-order rate constant was obtained by a linear plot of  $k_{\text{obs}}$  ( $\text{s}^{-1}$ ) vs glutathione concentration ( $R = 0.999$ ). <sup>c</sup> The rate of oxoMn(IV) reduction by Trolox was obtained by a second-order kinetic analysis of the experimental data from a stoichiometric reaction between oxoMn(IV) and Trolox in a double-mixing stopped-flow experiment analogous to that described for ascorbate (plot of  $(A_0 - A_\infty)/(A - A_\infty)$  vs time,  $R = 0.996$ ).

(Figure 2b). Curiously, though the rate-limiting step in the catalytic decomposition of  $\text{ONOO}^-$  is the oxoMn(IV) formation with a second-order rate constant of  $1.8 \times 10^6 \text{ M}^{-1} \text{ s}^{-1}$ ,  $k_c$  for the Mn(III)TMPyP-glutathione redox couple is slightly higher than expected. This may be due to the acceleration of oxoMn(IV) formation by the trans-effect if the axial ligand of the manganese porphyrin is the thiolate of glutathione instead of a water molecule. The estimated  $k_c$  for the Mn(III)TMPyP-Trolox redox couple is slower than expected because of residual interference from the Trolox phenoxyl radical and quinone interconversion.

**Protection Against Oxidation and Nitration by Peroxynitrite.** Significantly, these Mn(III)TMPyP-antioxidant redox-coupled systems completely protected *all-trans*-retinoic acid (RA) in phospholipid vesicles from  $\text{ONOO}^-$  oxidation. Addition of 250  $\mu\text{M}$   $\text{ONOO}^-$  to 40  $\mu\text{M}$  RA in small unilamellar vesicles resulted in a complete loss of the RA chromophore, indicating oxidation (Figure 4a). At concentrations as low as 2  $\mu\text{M}$ , Mn(III)TMPyP redox coupled with 300  $\mu\text{M}$  ascorbate protected 99% of the RA chromophore from  $\text{ONOO}^-$  oxidation. Further, the Mn(III)TMPyP-antioxidant redox couples also prevented metal-catalyzed nitration of phenols by  $\text{ONOO}^-$  (Figure 4b). Reaction of 1 mM  $\text{ONOO}^-$  with 1 mM 4-hydroxyphenylacetic acid (HPA) in the presence of 5  $\mu\text{M}$  Mn(III)TMPyP yielded 37% of 4-hydroxy-3-nitrophenylacetic acid (nitro-HPA). Addition of ascorbate, Trolox, or glutathione offered dose-dependent protection of HPA. The presence of 2 equiv (2 mM) of the antioxidants completely prevented the nitration of HPA by  $\text{ONOO}^-$ . Interestingly, the efficacy of these biological antioxidants in preventing phenolic nitration followed a trend similar to that of their reduction of oxoMn(IV).

**Mn(III)TMPyP-Catalyzed Superoxide Dismutation.** The SOD activity of Mn(III)TMPyP was evaluated by directly observing the decay of  $\text{O}_2^{\bullet -}$  at 245 nm<sup>28</sup> by using a specialized four-syringe setup of the stopped-flow spectrophotometer, as described in the Experimental Section. In the absence of Mn(III)TMPyP, self-dismutation of  $\text{O}_2^{\bullet -}$  at pH 7.4 in 50 mM phosphate buffer was second order in  $\text{O}_2^{\bullet -}$  with a rate constant ( $k_{\text{self}}$ ) of  $7.34 \times 10^5 \text{ M}^{-1} \text{ s}^{-1}$  (Figure 5a), which is typical for  $\text{H}^+$ -catalyzed dismutation.<sup>5,22,28,29</sup> The decay of  $\text{O}_2^{\bullet -}$  was significantly accelerated by the introduction of Mn(III)TMPyP at low concentrations (Figure 5b). Taking into consideration both the self-dismutation and the Mn(III)TMPyP-catalyzed

(28) Riley, D. P.; Rivers, W. J.; Weiss, R. H. *Anal. Biochem.* **1991**, *196*, 344.

(29) Bielski, B. H. J. *Photochem. Photobiol.* **1978**, *28*, 645.

(27) Buettner, G. R. *Arch. Biochem. Biophys.* **1993**, *300*, 535.

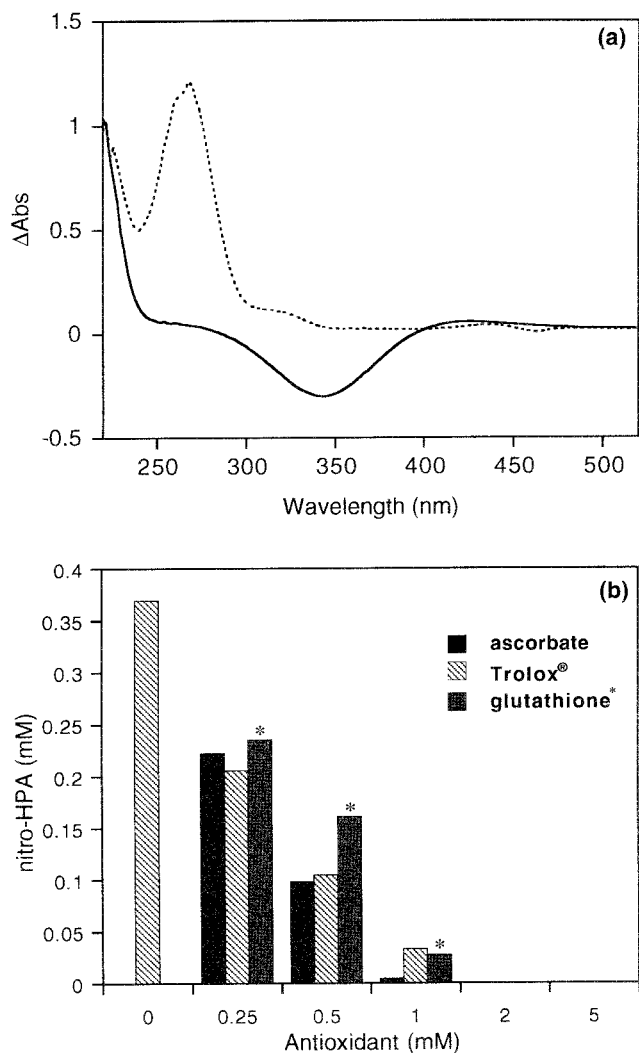


**Figure 4.** Protection against oxidation and nitration by peroxyntirite. (a) Difference UV-vis spectra: the solid trace shows the reaction of 250  $\mu\text{M}$  ONOO<sup>-</sup> with 40  $\mu\text{M}$  *all-trans*-retinoic acid in small unilamellar vesicles, while the dotted trace shows the same reaction but in the presence of 2  $\mu\text{M}$  Mn(III)TMPyP and 300  $\mu\text{M}$  ascorbate. Each difference spectrum is obtained by subtraction of a spectrum measured after addition of ONOO<sup>-</sup> (and ascorbate) from a spectrum measured before addition of ONOO<sup>-</sup>. (b) HPLC analysis of nitro-HPA produced in the reactions of 1 mM HPA and 1 mM ONOO<sup>-</sup> in the presence of 5  $\mu\text{M}$  Mn(III)TMPyP and various concentrations (0, 0.25, 0.5, 1, 2, 5 mM) of ascorbate, glutathione\*, or Trolox.

dismutation, the rate of O<sub>2</sub><sup>•-</sup> decomposition can be expressed as eq 1

$$-d[\text{O}_2^{\bullet-}]/dt = k_{\text{self}}[\text{O}_2^{\bullet-}] + k_{\text{obs}}[\text{O}_2^{\bullet-}] \quad (1)$$

in which

$$k_{\text{obs}} = k_c[\text{Mn(III)TMPyP}] \quad (2)$$

Integration of eq 1 yields the following expression for the concentration of O<sub>2</sub><sup>•-</sup> with time.

$$[\text{O}_2^{\bullet-}] = \frac{[\text{O}_2^{\bullet-}]_0 k_{\text{obs}} \exp(-k_{\text{obs}}t)}{k_{\text{obs}} + k_{\text{self}}[\text{O}_2^{\bullet-}]_0(1 - \exp(-k_{\text{obs}}t))} \quad (3)$$

The set of first-order rate constants,  $k_{\text{obs}}$ , was extracted by nonlinear least-squares fitting of the experimental data into eq

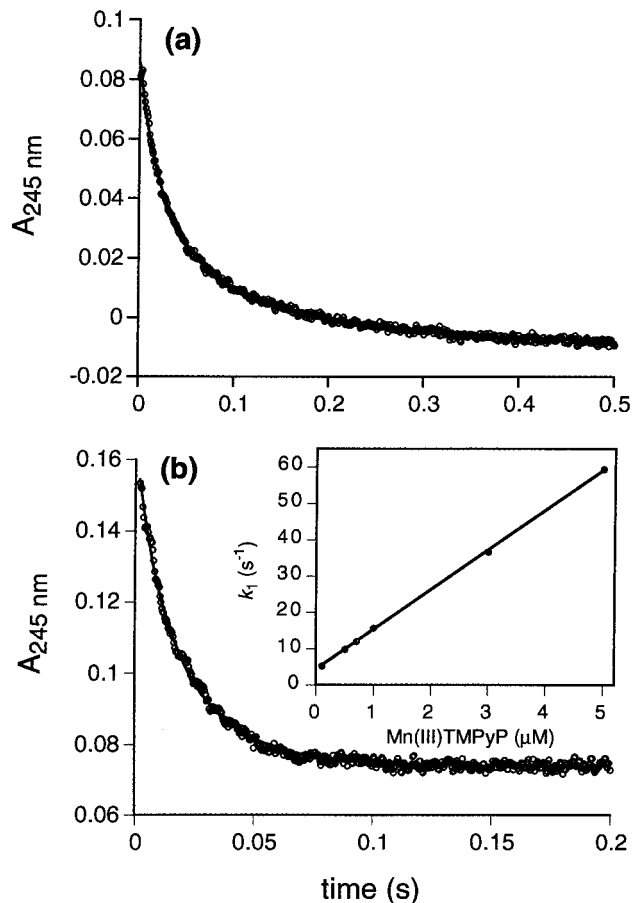


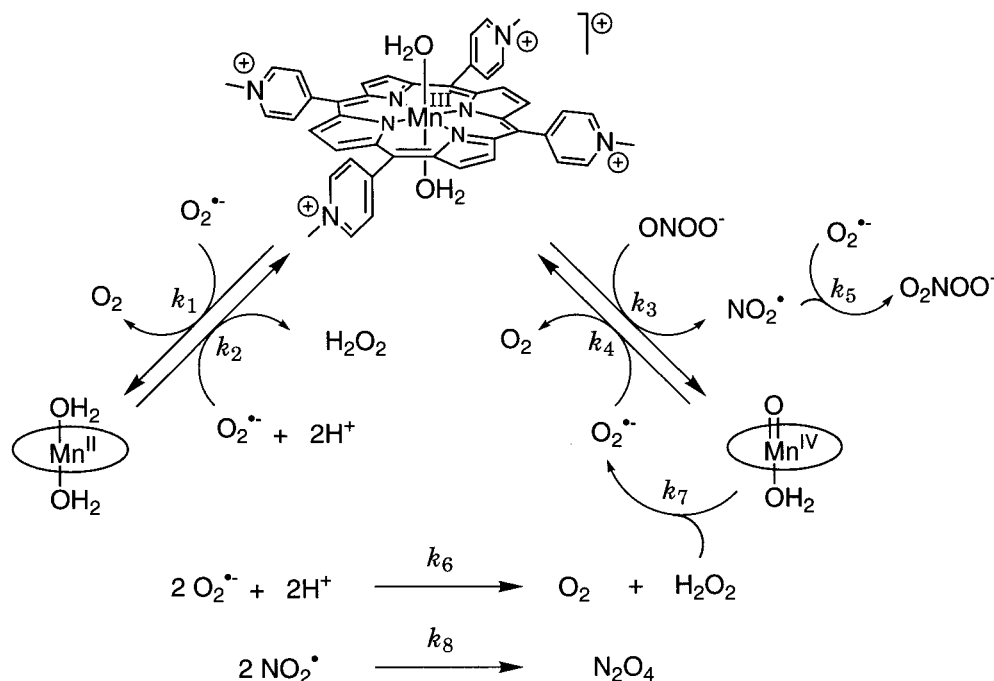
**Figure 5.** Decay of O<sub>2</sub><sup>•-</sup> in 50 mM, pH 7.4 phosphate buffer at 25 °C (a) in the absence of porphyrin and (b) in the presence of 3  $\mu\text{M}$  Mn(III)TMPyP. The solid lines in (a) and (b) are the nonlinear least-squares fitting of the experimental data into second-order kinetics ( $R = 0.999$ ) and eq 3 ( $R = 0.997$ ), respectively. Inset: Linear least-squares fit of the pseudo-first-order rate constants vs Mn(III)TMPyP concentrations ( $R = 0.999$ ).

3. A typical trace is shown in Figure 5b. The catalytic rate constant of Mn(III)TMPyP-catalyzed dismutation of O<sub>2</sub><sup>•-</sup> is  $1.1 \times 10^7 \text{ M}^{-1} \text{ s}^{-1}$ , determined from the slope of a linear plot of  $k_{\text{obs}}$  vs Mn(III)TMPyP concentrations (Figure 5b inset). This rate is in agreement with the results obtained by indirect assay<sup>17</sup> and pulse radiolysis.<sup>22</sup> The presence of ascorbate did not affect the observed rate of Mn(III)TMPyP-catalyzed dismutation of O<sub>2</sub><sup>•-</sup>. The SOD activity of an anionic manganese porphyrin, MnTBAP, was also examined. Mn(III)TBAP was inefficient in decomposing O<sub>2</sub><sup>•-</sup>, with a catalytic rate slower than the rate of O<sub>2</sub><sup>•-</sup> self-dismutation, which represents the lower limit of the stopped-flow method.

Mn(III)TMPyP effects the dismutation of O<sub>2</sub><sup>•-</sup> via a rate-limiting reduction ( $k_1$ ) of Mn(III) to Mn(II) and a fast oxidation ( $k_2$ ) of Mn(II) back to Mn(III),<sup>22</sup> as shown in Scheme 2.

Accordingly, Mn(III)TMPyP remained in the Mn(III) oxidation state during the entire course of O<sub>2</sub><sup>•-</sup> dismutation, as determined by monitoring the porphyrin absorbance at 462 nm. The Mn(II) species can be considered a transient reactive intermediate, since the oxidation of Mn(II) by O<sub>2</sub><sup>•-</sup>, with an estimated rate constant of  $\sim 4 \times 10^9 \text{ M}^{-1} \text{ s}^{-1}$ ,<sup>22</sup> is almost 3 orders of magnitude faster than the reduction of Mn(III) by O<sub>2</sub><sup>•-</sup>. Applying a steady-state approximation to the intermediate Mn(II) species,  $k_{\text{obs}}$  can be expressed as eq 4.

$$k_{\text{obs}} = 2k_1[\text{Mn(III)TMPyP}] \quad (4)$$

Scheme 2<sup>a</sup>

<sup>a</sup>  $k_1 = 5.5 \times 10^6 \text{ M}^{-1} \text{ s}^{-1}$ ;  $k_2 = 4 \times 10^9 \text{ M}^{-1} \text{ s}^{-1}$ ;  $k_3 = 1.16 \times 10^6 \text{ M}^{-1} \text{ s}^{-1}$ ;  $k_4 = 1 \times 10^8 \text{ M}^{-1} \text{ s}^{-1}$ ;  $k_5 = 4.5 \times 10^9 \text{ M}^{-1} \text{ s}^{-1}$ ;  $k_6 = 7.34 \times 10^5 \text{ M}^{-1} \text{ s}^{-1}$ ;  $k_7 = 1.17 \times 10^3 \text{ M}^{-1} \text{ s}^{-1}$ ;  $k_8 = 9 \times 10^8 \text{ M}^{-1} \text{ s}^{-1}$ . As described in the text and figure legends, the rates  $k_1$ ,  $k_3$ ,  $k_4$ , and  $k_6$  were determined at 23 °C in ~8% DMSO/50 mM phosphate buffer, pH 7.4, while  $k_7$  was determined at 23 °C in 50 mM phosphate buffer, pH 7.4. The values for the remaining rates ( $k_2$ ,<sup>22</sup>  $k_5$ ,<sup>22</sup> and  $k_8$ <sup>33</sup>) are taken from the literature.

Thus,

$$k_1 = k_2/2 = 5.5 \times 10^6 \text{ M}^{-1} \text{ s}^{-1} \quad (5)$$

**Superoxide-Coupled Mn(III)TMPyP Reduction of Peroxynitrite.** The fast reduction of Mn(III) to Mn(II) by  $\text{O}_2^{\bullet-}$  suggested that  $\text{O}_2^{\bullet-}$ , like the biological antioxidants, would also rapidly reduce oxoMn(IV) to Mn(III). Accordingly, we designed an experiment to determine whether  $\text{O}_2^{\bullet-}$  could drive the reduction of  $\text{ONO}_2^-$  in the presence of Mn(III)TMPyP.

First, the direct reaction of oxoMn(IV) with  $\text{O}_2^{\bullet-}$  was monitored by stopped-flow spectrophotometry (Figure 6a) to confirm our expectation that  $\text{O}_2^{\bullet-}$  would rapidly reduce oxoMn(IV) to Mn(III). Indeed, this reduction rate was at the upper detection limit of the stopped-flow spectrophotometer, even for the near stoichiometric reaction of 5  $\mu\text{M}$  oxoMn(IV) with ~5–10  $\mu\text{M}$   $\text{KO}_2$ . However, from the data in Figure 6a, the second-order rate constant could be estimated to be on the order of  $1 \times 10^8 \text{ M}^{-1} \text{ s}^{-1}$ . Therefore, this fast reduction of oxoMn(IV) by  $\text{O}_2^{\bullet-}$  could turn over the cycle of Mn(III)TMPyP-catalyzed decomposition of  $\text{ONO}_2^-$ , which is again limited by the rate of generation of oxoMn(IV) by  $\text{ONO}_2^-$  (Scheme 2). In the less polar medium in which these experiments were conducted (~8% DMSO/pH 7.4, 50 mM phosphate buffer), oxidation of Mn(III) to oxoMn(IV) by  $\text{ONO}_2^-$  has a rate constant of  $1.16 \times 10^6 \text{ M}^{-1} \text{ s}^{-1}$  (Figure 6b), which is slightly slower than that in pure phosphate buffer.<sup>30</sup>

The reduction rate of oxoMn(IV) by  $\text{H}_2\text{O}_2$ , the dismutation product of  $\text{O}_2^{\bullet-}$ , was also measured by double-mixing stopped-flow experiments, which gave a second-order rate constant of  $1.17 \times 10^3 \text{ M}^{-1} \text{ s}^{-1}$ . This result served to limit the significance of a peroxide-dependent cycle, and was an important control since  $\text{H}_2\text{O}_2$  is the major impurity in the  $\text{ONO}_2^-$  stock solutions.

(30) This is consistent with our proposition that heterolytic cleavage of the  $\text{ONO}_2^-$  O–O bond to generate oxoMn(V) is followed by fast one-electron  $\text{NO}_2^-$  reduction to form oxoMn(IV) (see refs 8 and 16).

To demonstrate  $\text{O}_2^{\bullet-}$ -coupled Mn(III)TMPyP reduction of  $\text{ONO}_2^-$ , we again employed the extended-plate, four-syringe setup of the stopped-flow spectrophotometer (described in the Experimental Section). However, we departed from the usual procedure for monitoring the dismutation of  $\text{O}_2^{\bullet-}$ , which involves loading  $\text{KO}_2/\text{DMSO}$  in the first syringe so that it mixes with buffer from the second syringe in the aging loop before reaching the detector cell. Instead, we loaded  $\text{ONO}_2^-$  in the first syringe, Mn(III)TMPyP in the second syringe, and  $\text{KO}_2/\text{DMSO}$  in the third syringe. As a result,  $\text{ONO}_2^-$  and Mn(III)TMPyP mixed in the aging loop, producing a mixture of oxoMn(IV) and the excess  $\text{ONO}_2^-$ , which then reacted with  $\text{O}_2^{\bullet-}$  in the detector cell.

With the use of this special setup, we monitored the reaction of 5  $\mu\text{M}$  Mn(III)TMPyP with 100  $\mu\text{M}$   $\text{ONO}_2^-$  and ~160  $\mu\text{M}$   $\text{O}_2^{\bullet-}$ ; the data are shown in Figure 7, trace a. As can be seen, the manganese porphyrin, monitored at 462 nm, was maintained as Mn(III) by rapid  $\text{O}_2^{\bullet-}$  reduction of oxoMn(IV) during the initial phase of the reaction (ca. 25 ms). Only after  $\text{O}_2^{\bullet-}$  had been fully consumed was Mn(III) oxidized by excess  $\text{ONO}_2^-$  to form oxoMn(IV). A control experiment in the absence of  $\text{O}_2^{\bullet-}$  showed very different behavior (Figure 7, trace c): only oxidation of Mn(III) by  $\text{ONO}_2^-$  was observed under these conditions. Taken together, these experiments show that Mn(III)TMPyP can act as a  $\text{O}_2^{\bullet-}$ -coupled  $\text{ONO}_2^-$  reductase, introducing a new pathway for  $\text{O}_2^{\bullet-}$  removal by Mn(III)TMPyP.

We present in Scheme 2 a mechanism for Mn(III)TMPyP-catalyzed  $\text{O}_2^{\bullet-}$  removal. In this bifurcated process, the left fork describes the usual Mn(III)–Mn(II) dismutation cycle, while the right fork describes the oxoMn(IV)–Mn(III)  $\text{ONO}_2^-$  reductase cycle. Furthermore,  $\text{O}_2^{\bullet-}$  can react with nitrogen dioxide ( $\text{NO}_2$ ) at the near diffusion-controlled rate of  $4.5 \times 10^9 \text{ M}^{-1} \text{ s}^{-1}$  to form peroxynitrate ( $\text{O}_2\text{NOO}^-$ )<sup>31</sup> in the right-hand fork of Scheme 2. A reassuring confirmation of this reaction

(31) Løgager, T.; Sehested, K. *J. Phys. Chem.* **1993**, *97*, 10047.

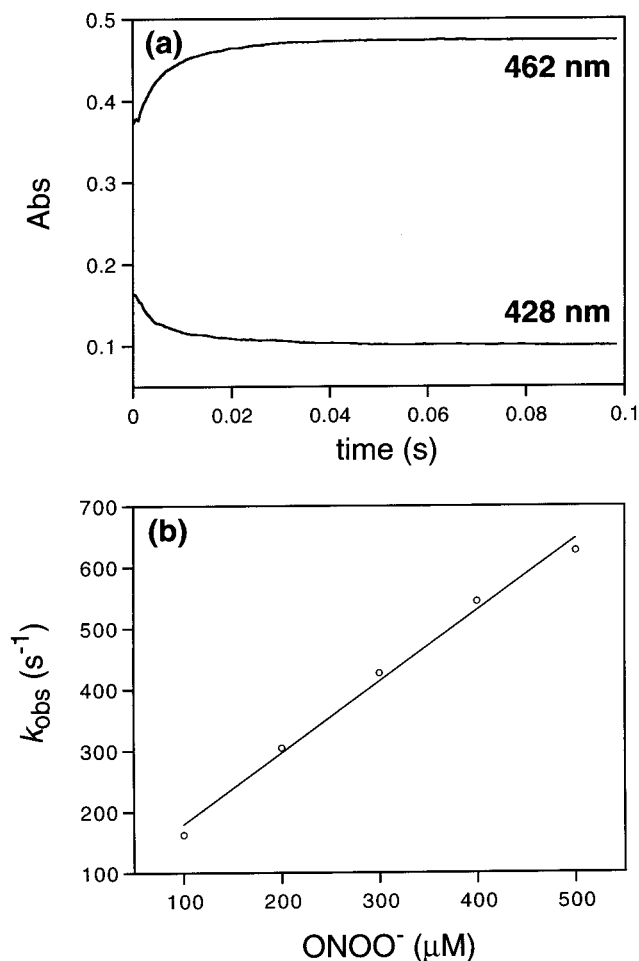


**Figure 6.** (a) The reduction of 5  $\mu\text{M}$  oxoMn(IV) by  $\sim 5\text{--}10\ \mu\text{M}$   $\text{O}_2^{\bullet-}$ . The oxoMn(IV) intermediate was prepared by the reaction of 5  $\mu\text{M}$  Mn(III)TMPyP with 5.5  $\mu\text{M}$   $\text{HSO}_5^-$ . The disappearance of oxoMn(IV) was monitored at 428 nm, and the reappearance of Mn(III) was monitored at 462 nm. (b) Linear plot of the first-order rate constants ( $k_{\text{obs}}$ ) of oxoMn(IV) formation vs ONOO<sup>-</sup> concentrations ( $R = 0.996$ ).

scheme derives from a simulation of the data. Taking into consideration all eight possible reactions shown in Scheme 2, with all eight rate constants individually determined, the simulated plot reproduced the experimental data with no adjustable parameters (Figure 7, trace b).

**Biological Implications.** Cells exist in a reducing environment rich in antioxidants. However, as we<sup>23</sup> and others<sup>26,32</sup> have shown, the reactions of ONOO<sup>-</sup> with these biological reductants are quite slow, indicating that antioxidants such as ascorbate, glutathione, and tocopherol alone cannot play a direct role in the defense against ONOO<sup>-</sup>. In fact, ONOO<sup>-</sup> readily oxidizes and nitrates proteins long before the endogenous antioxidants have been depleted in human plasma.<sup>33</sup> By contrast, we have shown that Mn(III)TMPyP can efficiently utilize ascorbate, glutathione, and Trolox as the electron source for the reduction of ONOO<sup>-</sup>. Thus, under normal conditions, the ONOO<sup>-</sup> reductase activity of Mn(III)TMPyP may protect cells from oxidative damage.

Conversely, under conditions of oxidative stress and depleted antioxidant levels, Mn(III)TMPyP can protect cells from both ONOO<sup>-</sup> and  $\text{O}_2^{\bullet-}$  mediated injury. Oxidative stress is the

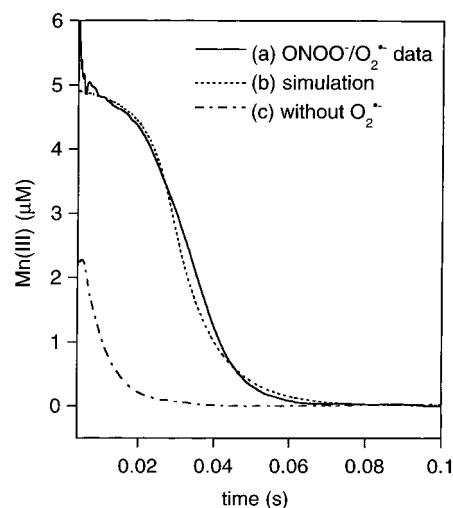


**Figure 7.** Reaction of 100  $\mu\text{M}$  ONOO<sup>-</sup>, 5  $\mu\text{M}$  Mn(III)TMPyP, and  $\sim 160\ \mu\text{M}$   $\text{O}_2^{\bullet-}$  (0.8 equiv based on ONOO<sup>-</sup> concentration). (a) The solid trace is the experimental data monitoring Mn(III) concentration. (b) The dotted trace is a kinetic simulation based on the eight possible reactions shown in Scheme 2, with no adjustable parameters. (c) The bottom trace is the same reaction as in (a), except in the absence of  $\text{O}_2^{\bullet-}$ .

consequence of imbalance in the cellular levels of prooxidants and antioxidants.<sup>34,35</sup> Excessive production of reactive oxygen species, including  $\text{O}_2^{\bullet-}$  and ONOO<sup>-</sup>, results in much lower concentrations and even depletion of antioxidants. Nevertheless, we have shown here that Mn(III)TMPyP has the potential to catalyze the concurrent removal of  $\text{O}_2^{\bullet-}$  and ONOO<sup>-</sup> under these pathological conditions.

In the new bifurcated mechanism for Mn(III)TMPyP-catalyzed elimination of  $\text{O}_2^{\bullet-}$  (Scheme 2), Mn(III)TMPyP performs both as a SOD mimic (left fork) and as a  $\text{O}_2^{\bullet-}$  coupled ONOO<sup>-</sup> reductase (right fork). It is instructive to consider the ramifications of these results in biological situations. The steady-state concentrations of  $\text{NO}^*$ ,  $\text{O}_2^{\bullet-}$ , and ONOO<sup>-</sup> under physiological conditions are highly tissue dependent. Physiological  $\text{NO}^*$  concentrations span 3 orders of magnitude, from the 5 nM required for guanylate cyclase activation to the  $\sim 4\ \mu\text{M}$  measured under conditions of cerebral ischemia.<sup>2,36</sup> Cellular SOD activity keeps the concentrations of  $\text{O}_2^{\bullet-}$  very low, with typical steady-state concentrations of  $\sim 10^{-10}\ \text{M}$ .<sup>3,37</sup> As for ONOO<sup>-</sup>, nanomolar concentrations were detected in agonist-induced endothelial cells.<sup>38</sup> Assuming the steady-state concentrations of  $\text{O}_2^{\bullet-}$  and ONOO<sup>-</sup> to be  $\sim 10^{-10}$  and  $\sim 4 \times 10^{-9}\ \text{M}$ , respectively, the manganese porphyrin catalyst inventory would be 60% Mn(III) and 40% oxoMn(IV) if the oxoMn(IV) concentration is treated as a steady state. Thus, the partition of  $\text{O}_2^{\bullet-}$  down the two forks of the bifurcated pathway shown in Scheme 2 can be evaluated as in eq 6, where  $[\text{O}_2^{\bullet-}]_{\text{L}}$  and  $[\text{O}_2^{\bullet-}]_{\text{R}}$  represent the concentrations of  $\text{O}_2^{\bullet-}$  decomposed through the left-hand and the right-hand forks, respectively.

$$\frac{[\text{O}_2^{\bullet-}]_{\text{L}}}{[\text{O}_2^{\bullet-}]_{\text{R}}} = \frac{k_1 \cdot [\text{Mn(III)}]}{k_4 \cdot [\text{Mn(IV)}]} = 0.08 \quad (6)$$

(34) Scandalios, J. G. *Oxidative Stress and the Molecular Biology of Antioxidant Defenses*; Cold Spring Harbor Laboratory Press: New York, 1997.

(35) Sies, H. *Oxidative Stress*; Academic: Orlando, 1985.

(36) Malinski, T.; Bailey, F.; Zhang, Z. G.; Chopp, M. J. *Cereb. Blood Flow Metab.* **1993**, *13*, 355.

(37) Gardner, P. R.; Fridovich, I. *J. Biol. Chem.* **1992**, *267*, 8757.

(32) Koppenol, W. H.; Moreno, J. J.; Pryor, W. A.; Ischiropoulos, H.; Beckman, J. S. *Chem. Res. Toxicol.* **1992**, *5*, 834.

(33) Van der Vliet, A.; Smith, D.; O'Neill, C. A.; Kaur, H.; Darley Usmar, V.; Cross, C. E.; Halliwell, B. *Biochem. J.* **1994**, *303*, 295.

Significantly, more than 90% of the  $O_2^{\bullet-}$  will be depleted via the ONOO<sup>-</sup>-coupled pathway, given the rate constants we have measured herein. Therefore, though Mn(III)TMPyP has only modest SOD activity, it could be expected to effectively remove  $O_2^{\bullet-}$  even in the absence of antioxidants in tissues under oxidative stress.

## Conclusions

We have shown that a water-soluble manganese porphyrin, Mn(III)TMPyP, can become an efficient peroxynitrite reductase when redox coupled with biological antioxidants, though the direct reactions of ONOO<sup>-</sup> with these antioxidants are slow. Further, these Mn(III)TMPyP-antioxidant redox couples protected membrane components from oxidation and protected phenols from nitration. Because cells exist in an environment replete with antioxidants, including vitamin C (ascorbate),<sup>39,40</sup> glutathione,<sup>41</sup> and vitamin E (tocopherol),<sup>42,43</sup> the ONOO<sup>-</sup> reductase reactivity of manganese porphyrins may play an important role in the protection of cells from oxidative stress in  $O_2^{\bullet-}$  and ONOO<sup>-</sup> related diseases.

We have measured the rate of Mn(III)TMPyP-catalyzed dismutation directly for the first time, using stopped-flow spectrophotometry. The catalytic rate constant we determined ( $1.1 \times 10^7 \text{ M}^{-1} \text{ s}^{-1}$ ) agrees well with the results obtained by indirect assay<sup>17</sup> and pulse radiolysis.<sup>22</sup> Further, we have determined that  $O_2^{\bullet-}$ , like the above-mentioned biological antioxidants, can rapidly reduce oxoMn(IV) to the Mn(III) oxidation state, transforming Mn(III)TMPyP into a  $O_2^{\bullet-}$ -coupled ONOO<sup>-</sup> reductase. Under the extreme conditions of oxidative stress and antioxidant depletion within a cell, the concomitant removal of both  $O_2^{\bullet-}$  and ONOO<sup>-</sup> mediated by the ONOO<sup>-</sup> reductase activity of Mn(III)TMPyP may become significant in the cell-protective mechanism of this and related metalloporphyrins.<sup>44</sup>

Finally, the dissection described herein of the mechanisms of the reactions of Mn(III)TMPyP with  $O_2^{\bullet-}$  and ONOO<sup>-</sup>, in the presence and absence of antioxidants, may have significant biological implications beyond elucidation of the cell-protective effects of the metalloporphyrins. ONOO<sup>-</sup> is known to react rapidly with a host of metalloenzymes, such as myeloperoxidase ( $k > 2 \times 10^6 \text{ M}^{-1} \text{ s}^{-1}$ ),<sup>25</sup> Cu,ZnSOD ( $k = 10^3\text{--}10^5 \text{ M}^{-1} \text{ s}^{-1}$ ),<sup>45</sup> MnSOD,<sup>46</sup> and P450-like enzymes such as nitric oxide synthase<sup>47</sup> and prostacyclin synthase,<sup>48</sup> and cytochrome *c*.<sup>49</sup> Thus, the reactions of  $O_2^{\bullet-}$  and ONOO<sup>-</sup> with MnTMPyP and other metalloporphyrins may provide an instructive model for understanding reactions of oxidants with these important biological targets.

## Experimental Section

**Materials.** 5,10,15,20-Tetrakis(*N*-methyl-4'-pyridyl)porphinatoman-ganese(III) chloride [Mn(III)TMPyP(Cl)] was purchased from Mid-Century Chemical. Anhydrous monosodium phosphate and anhydrous

disodium phosphate were purchased from Sigma. Sodium l-ascorbate, Trolox, glutathione, *all-trans*-retinoic acid, 4-hydroxyphenylacetic acid, potassium superoxide (KO<sub>2</sub>), potassium peroxymonosulfate (HSO<sub>5</sub><sup>-</sup>), and 4,4',4''',4''''-(2*H*,23*H*-porphine-5,10,15,20-tetraaryl)tetrakis(benzoic acid) (H<sub>2</sub>TBAP) were obtained from Aldrich. Mn(III)TBAP(Cl) was prepared by metalation of H<sub>2</sub>TBAP under standard conditions.<sup>50</sup> Peroxynitrite was prepared from the reaction of acidic H<sub>2</sub>O<sub>2</sub> with sodium nitrite following the published procedure.<sup>16</sup> All the solvents were analytical grade. Dry DMSO was distilled under reduced pressure from calcium hydride. Water used in all the experiments was distilled and deionized (Millipore, Milli-Q).

**Kinetics of Peroxynitrite Decomposition.** The kinetic profiles of Mn(III)TMPyP-catalyzed decomposition of ONOO<sup>-</sup> in 25 mM phosphate pH 7.4 buffer at 25 °C were recorded on a HI-TECH SF-61 DX2 rapid-mixing stopped-flow spectrophotometer. In the presence of fixed concentrations of ascorbate (150 μM), glutathione (2 mM), or Trolox (150 μM), the porphyrin concentration was varied from 2 to 15 μM. The decay of ONOO<sup>-</sup> (100 μM) was monitored at 302 nm. In a similar experiment, the rate of reaction of Mn(III)TBAP and ascorbate (150 μM) with ONOO<sup>-</sup> (100 μM) was found to be about 40 times slower than that of Mn(III)TMPyP/ascorbate:  $k_c = 5.0 \times 10^4 \text{ M}^{-1} \text{ s}^{-1}$ , obtained from the slope of a linear plot of  $k_{\text{obs}}$  vs Mn(III)TBAP concentrations ( $R = 0.999$ ). The reduction rates of oxoMn(IV) intermediates by antioxidants (ascorbate, glutathione, or Trolox) were measured directly by performing double-mixing experiments: the oxoMn(IV) intermediates were fully generated by HSO<sub>5</sub><sup>-</sup> during the first mixing step, and then the antioxidant was added in the second mixing step. The recovery of Mn(III)TMPyP and the disappearance of oxoMn(IV) complexes were monitored at 462 and 428 nm, respectively.

**Protection Against Oxidation and Nitration.** Small unilamellar vesicles (SUV) containing 40 μM *all-trans*-retinoic acid (RA) were prepared following the literature procedure.<sup>51</sup> The membrane-bound substrate was mixed with 250 μM ONOO<sup>-</sup>, and the extent of oxidation was evaluated as the decrease in absorbance at 340 nm of the RA chromophore. Protection of RA oxidation was attempted by adding Mn(III)TMPyP (2, 5, and 10 μM) in conjunction with ascorbate (300 μM). Reaction of 1 mM ONOO<sup>-</sup> with 1 mM HPA in the presence of 5 μM Mn(III)TMPyP produced nitro-HPA, which was quantitated by reverse-phase HPLC analysis (Waters Delta PAK 5 μ C18 300 Å column; gradient of methanol and 5 mM pH 7.4 phosphate buffer (v/v): 10:95 at 0 min, 40:60 at 10 min). Ascorbate, Trolox, or glutathione (0.25, 0.5, 1, 2, 5 mM) was added to the reaction mixtures to prevent the nitration of HPA.

**Superoxide Dismutation.** A DMSO solution of KO<sub>2</sub> (~2 mM) was prepared following the published procedure.<sup>28</sup> The dismutation of  $O_2^{\bullet-}$  was monitored directly at the  $O_2^{\bullet-}$  absorbance (245 nm), using a special setup of the four-syringe, double-mixing sample-handling unit to reduce changes in the refractive index due to the mixing of DMSO and buffers.<sup>52</sup> In this stopped-flow setup, the KO<sub>2</sub>/DMSO solution was loaded in syringe A (0.5 mL) and 50 mM pH 7.4 phosphate buffer was loaded in syringes B (2.5 mL), C (0.5 mL), and D (2.5 mL) (syringes A, B, C, and D were labeled from left to right). All four syringes were pushed up simultaneously by the extended plate; the contents of syringes A and B were first mixed in an aging loop, and then mixed with the contents of syringes C and D. A 12-fold dilution of the KO<sub>2</sub>/DMSO solution was achieved by using this two-stage mixing, thus minimizing the interference due to DMSO/water interaction. In the SOD activity assays, manganese porphyrin solutions (either Mn(III)TMPyP or Mn(III)TBAP) were loaded into syringe C.<sup>53</sup>

For the  $O_2^{\bullet-}$ -coupled ONOO<sup>-</sup> reduction experiment, ONOO<sup>-</sup>, Mn(III)TMPyP, KO<sub>2</sub>/DMSO, and 50 mM pH 7.4 phosphate buffer were placed in syringes A, B, C, and D, respectively. Though the four syringes were pushed up simultaneously by an extended plate, ONOO<sup>-</sup>

(38) Kooy, N. W.; Royall, J. A. *Arch. Biochem. Biophys.* **1994**, *310*, 352.

(39) Margolis, S. A.; Davis, T. *Clin. Chem.* **1988**, *34*, 2217.

(40) Behrens, W. A.; Madère, R. *Anal. Biochem.* **1987**, *165*, 102.

(41) Stryer, L. *Biochemistry*, 4th ed.; W. H. Freeman and Company: New York, 1995; p 731.

(42) Sies, H.; Murphy, M. E. *J. Photochem. Photobiol.* **1991**, *B*, 8, 211.

(43) Burton, G. W.; Traber, M. G. *Annu. Rev. Nutr.* **1990**, *10*, 357.

(44) Hunt, J. A.; Lee, J.; Groves, J. T. *Chem. Biol.* **1997**, *4*, 845.

(45) Gryglewski, R. J.; Palmer, R. M. J.; Moncada, S. *Nature* **1986**, *320*, 454.

(46) MacMillan-Crow, L. A.; Crow, J. P.; Kerby, J. D.; Beckman, J. S.; Thompson, J. A. *Proc. Natl. Acad. Sci. U.S.A.* **1996**, *93*, 11853.

(47) Pasquet, J. P. E. E.; Zou, M. H.; Ullrich, V. *Biochimie* **1996**, *78*, 785.

(48) Zou, M. H.; Ullrich, V. *FEBS Lett.* **1996**, *382*, 101.

(49) Thomson, L.; Trujillo, M.; Telleri, R.; Radi, R. *Arch. Biochem. Biophys.* **1995**, *319*, 491.

(50) Groves, J. T.; Neumann, R. *J. Am. Chem. Soc.* **1989**, *111*, 2900.

(51) Huang, C. *Biochemistry* **1969**, *8*, 344.

(52) See Hi-Tech Scientific Application Note AN.010.S60 for more detail.

(53) Forni, L. G.; Mora-Arellano, V. O.; Packer, J. E.; Willson, R. L. *J. Chem. Soc., Perkin Trans. 2* **1986**, *1*.

was first mixed with Mn(III)TMPyP in an aging loop to form oxoMn(IV)TMPyP, and then mixed with KO<sub>2</sub>/DMSO. Significant mixing artifacts at the beginning of the kinetic traces (~5 ms) were observed because the KO<sub>2</sub>/DMSO solution did not go through the aging loop to mix with buffer first. As a control experiment, the reaction of 100 μM ONOO<sup>-</sup> and ~160 μM O<sub>2</sub><sup>•-</sup> was monitored. The presence of the O<sub>2</sub><sup>•-</sup> did not significantly affect the rate of decomposition of ONOO<sup>-</sup>, suggesting that this reaction is slower than the self-dismutation of O<sub>2</sub><sup>•-</sup> under the experimental conditions.

To determine the significance of H<sub>2</sub>O<sub>2</sub>-dependent ONOO<sup>-</sup> reduction, the reduction rate of the oxoMn(IV) intermediate by H<sub>2</sub>O<sub>2</sub> was measured in a double-mixing experiment analogous to those described above for the antioxidants. The oxoMn(IV) intermediate was generated by mixing 5 μM Mn(III)TMPyP with 5 μM HSO<sub>5</sub><sup>-</sup> in the first mixing step. After a 5 s age time, addition of H<sub>2</sub>O<sub>2</sub> under pseudo-first-order conditions in the second mixing step resulted in the reduction of oxoMn(IV) to Mn(III). The second-order rate constant was obtained from the linear plot

of the first-order rate constants,  $k_{\text{obs}}$  (s<sup>-1</sup>), vs H<sub>2</sub>O<sub>2</sub> concentrations ( $R = 0.999$ ).

Reaction kinetics were simulated by using the Chemical Kinetics Simulator developed by IBM Almaden Research Center. The general settings for the simulation shown in Figure 7 are as follows: total number of molecules = 10<sup>8</sup>; record state at interval = 75; random number seed = 12947.

**Acknowledgment.** Support of this research by the National Institutes of Health (GM36928), the National Science Foundation for the purchase of 500 and 600 MHz NMR spectrometers, and Princeton University for the purchase of a stopped-flow spectrophotometer are gratefully acknowledged. We acknowledge the excellent technical assistance of Steven C. Tizio. J.A.H. is the recipient of an NIH NRSA fellowship (GM18490).

JA9801036